



# Temporal analysis on quantitative attribution of karst soil erosion: A case study of a peak-cluster depression basin in Southwest China

Jiangbo Gao<sup>a,\*</sup>, Huan Wang<sup>a,b,1</sup>

<sup>a</sup> Key Laboratory of Land Surface Pattern and Simulation, Institute of Geographic Sciences and Natural Resources Research, Chinese Academy of Sciences, Beijing, China

<sup>b</sup> College of Resources and Environment, University of Chinese Academy of Sciences, Beijing, China

## ARTICLE INFO

### Keywords:

Karst soil erosion  
Quantitative attribution  
Modified RUSLE  
Geographical detector  
Temporal dynamics  
China

## ABSTRACT

In karst areas, soil erosion is a significant problem, seriously impeding sustainable socioeconomic development. A thorough understanding and quantitative identification of the influencing factors are essential for soil erosion protection and rocky desertification management. This study identifies the dominant factors (and interactions) influencing soil erosion and its spatiotemporal variability in a karst basin, the Sancha River Basin, China. The geographical detector method was used to conduct the quantitative attribution analysis, based on the modified universal soil loss equation model for karst environments. The results revealed that karst soil erosion exhibited a notable decreasing trend over the past 36 years ( $p < 0.01$ ), decreasing from  $16.70 \text{ t ha}^{-1} \text{ a}^{-1}$  in 1980 to  $12.22 \text{ t ha}^{-1} \text{ a}^{-1}$  in 2015. The geographical detector results indicated significant differences in the strength of the association between influencing factors (or factor combinations) and karst soil erosion. Land use type was the dominant factor, followed by slope; a combination of land use type and slope was the dominant interaction factor, explaining at least 74% of the karst soil erosion distribution. Land use change dominated karst soil erosion dynamics in the 1980s and 1990s, and rainfall variability dominated in the 2000s. In addition, karst soil erosion showed high spatial heterogeneity, and the strength of the association differed substantially among diverse geomorphological types due to differences in the inner characteristics of each. These findings suggest that the characteristics of different geomorphological types should be considered for effective management and prevention of soil erosion at a regional level, and that steep croplands, especially with slopes higher than  $15^\circ$ , should be prohibited in karst areas. The methodology and framework can be used to better understand the relationships between soil erosion and its influencing factors in karst areas.

## 1. Introduction

Soil erosion is a global environmental and ecological problem (Borrelli et al., 2017; Martínez-Casasnovas et al., 2016), severely impeding sustainable socioeconomic development (Kefi et al., 2011). On-site and off-site problems related to soil erosion have been observed (Guo et al., 2015), including loss of soil productivity, water pollution, eutrophication and turbidity, flooding, and landslides (Ouyang et al., 2010; Vanacker et al., 2003; Yao et al., 2016). Determining the influencing mechanisms of soil erosion is instrumental for managing this problem. In karst areas, soil erosion is the main factor causing rocky desertification (Wang, 2003), but highly complex geological structures, diverse topography, and humid climates hinder soil erosion control (Tian et al., 2016; Febles-Gonzalez et al., 2012; Feng et al., 2016). Several studies have concentrated on karst soil erosion assessment and

the identification of driving forces, including rainfall, terrain, vegetation cover, land use type, soil physical properties, and other factors (Xu and Long, 2005; Yan et al., 2017; Xu and Peng, 2008; Zheng and Wang, 2016). For example, Febles-Gonzalez et al. (2012) noted that soil losses surpassed the permissible erosion threshold in karst regions of Havana, Cuba; Peng and Wang (2012) found that soil loss exhibited significant variation under different rainfall and land use regimes, and; Xiong et al. (2012) confirmed that geomorphology controls soil erosion at a macroscopic scale. Although most studies have identified one or more influencing factors of soil erosion, quantitative attribution analyses of single and multiple interacting factors are lacking. These analyses are an urgent and basic requirement for researchers and policy makers to develop soil protection measures for karst areas.

Understanding the dynamic principles of soil erosion under long-term data series is the basis for its effective control (Irvem et al., 2007;

\* Corresponding author at: No. 11A Datun Road, Chaoyang District, Beijing, China.

E-mail address: [gaojiangbo@igsnr.ac.cn](mailto:gaojiangbo@igsnr.ac.cn) (J. Gao).

<sup>1</sup> First co-author contributed equally to this work.

Ouyang et al., 2010). Temporal variability in soil erosion may be affected by the compensation effect, which is the alternation of events that transport sediment (source-limited) with those that break down the sediment (transport-limited regimes) (Kim et al., 2016). In addition, the frequency, magnitude, and specific sequence of the driving climatological events increase the uncertainty of erosion estimates (Campbell, 1992). However, few studies have stressed the importance of the temporal scale for soil erosion (Boix-Fayos et al., 2006), and most research has been conducted for only limited periods (< 10 years). In karst areas, most studies have performed investigations of soil erosion evolution with scattered time points (Zeng et al., 2011). For example, Zeng et al. (2017) recently studied the soil erosion evolution in karst geomorphology in southwest China in 2000, 2005, and 2013. However, studies based on discontinuous time series may inaccurately reflect the characteristics of soil erosion change. Hence, dynamic simulations of soil erosion and the identification of the determinants of soil erosion variability are necessary.

Karst soil erosion can be estimated using several methods, such as runoff field monitoring (Peng and Wang, 2012), runoff plot experiments (Dai et al., 2017), isotopic tracing (Bai et al., 2013) and mathematical models (Zeng et al., 2017). Among these methods, models are most appropriate for simulating soil erosion at a relatively large spatial scale. The revised universal soil loss equation (RUSLE), a popular empirical model, has been widely used in low-slope regions as well as for complex topographical landscape units (Sun et al., 2013; Zeng et al., 2017). The RUSLE model has also been used extensively in karst areas, such as southwest China (Chen et al., 2017; Feng et al., 2016; Li et al., 2016) and Cuba (Febles-Gonzalez et al., 2012). However, these applications ignored karst features, including less erodible soil in areas with severe rocky desertification, and erosion-resistant bedrock outcrops, and thus may have overestimated karst soil erosion (Feng et al., 2016; Zeng et al., 2017). Slow soil formation rates and severe soil erosion cause rocky desertification, which is characterized by extensive exposure of basement rocks (Wang et al., 2004). Outcropping bedrock can absorb rainfall after long-term weathering, and reduce the surface runoff velocity (Xiong et al., 2012). Further, underground infiltration and the resistance of outcropping bedrock cause discontinuous overland flow and sediment deposition patterns (Feng et al., 2016). Due to this discontinuity, the slope length ( $L$ ) factor may be smaller for karst areas than non-karst areas. Hence, the RUSLE model should be calibrated to accurately simulate karst soil erosion by considering outcropping bedrock and rocky desertification.

The goal of this study is to identify the dominant factors influencing soil erosion and temporal variability in karst areas in southwest China. To achieve this goal, we performed the following analyses: (1) calibration of the RUSLE model for karst areas by considering karst rocky desertification, and discontinuous surface runoff caused by outcropping bedrock; (2) quantitative identification of the dominant factors affecting the distribution of soil erosion, and (3) quantitative evaluation of the dominant factors affecting the variability of soil erosion.

## 2. Methods

### 2.1. Study area

The study area, the Sancha River Basin (SRB), is located in Guizhou Province, southwest China (Fig. 1), with an area of 4860 km<sup>2</sup>. The Sancha River, with a length of 325.6 km, is a first order tributary of the Wujiang River. The basin is characterized by karst peak-cluster depressions, where carbonate is widely distributed. It experiences a subtropical monsoon climate, with rainfall concentrated between May and October, and has an annual mean rainfall of 1100 mm. The changing climate, complex topography, and high levels of human activity make the ecosystem highly fragile. Unsustainable land use combined with the fragility of the ecosystem cause serious rocky desertification, and rocky desertification with thin soil overlying bedrock is a common landscape

in this area.

### 2.2. Data

The RUSLE model requires both environmental and anthropogenic data, including rainfall, a digital elevation model (DEM), a soil dataset, and land use type. Rainfall data from 1980 to 2015 were acquired from the National Meteorological Information Center (<http://data.cma.cn>). A raster gridded yearly rainfall dataset was interpolated using the ANUSPLIN 4.2 software (Hutchinson, 2001) with data from 28 meteorological stations in the SRB and its surrounding areas. A high-resolution DEM (9 m, Google Earth ver. 6.0.3) was applied to simulate the topographic factor. The soil dataset, including soil type and physical properties at a 1-km spatial resolution, was obtained from the Harmonized World Database ver. 1.1 established by the Food and Agriculture Organization of the United Nations and the International Institute for Applied System Analysis. The data set was provided by the Cold and Arid Regions Sciences Data Center at Lanzhou, China (<http://westdcwestgis.ac.cn>). Land use data (30-m resolution) for the years 1980, 1990, 1995, 2000, 2005, 2010 and 2015, were provided by the Data Center for Resources and Environmental Sciences, Chinese Academy of Sciences (RESDC) (<http://www.resdc.cn>). In addition, lithology and geomorphology data were used to explore the power of the determinant for soil erosion from data acquired by the RESDC. The lithology map was classified into ten types (Fig. S1a) and the geomorphology was classified into five types (Fig. S1b, Table S1). Rocky desertification data were provided by the State Forestry Administration (<http://www.forestry.gov.cn/>).

### 2.3. Methods

#### 2.3.1. The RUSLE model

The RUSLE model (Renard et al., 1997), revised from the USLE model (Wischmeier and Smith, 1978), has been widely used to simulate soil erosion worldwide, supported by GIS and remote sensing methods. The equation is as follows:

$$A = R \times K \times LS \times C \times P \quad (1)$$

where  $A$  is the annual soil erosion module ( $t\ ha^{-1}\ a^{-1}$ ),  $R$  is the rainfall erosivity factor ( $MJ\ mm\ ha^{-1}\ h^{-1}\ a^{-1}$ ),  $K$  is the soil erodibility factor ( $t\ hm^2\ h\ MJ^{-1}\ mm^{-1}\ hm^{-2}$ ),  $LS$  is the slope aspect factor,  $C$  is the land cover and management factor, and  $P$  is the conservation measure factor.

The RUSLE model does not differentiate between the enough erodible soil areas and the less erodible soil areas (serious rocky desertification areas) and thus usually overestimates the results in karst areas, requiring modification to improve its accuracy with regard to less erodible soil in serious rocky desertification areas (Xiong et al., 2012). A previous study showed that increased bedrock bareness results in decreased soil erosion (Wang et al., 2010b). This can be explained by the following factors a) outcropping bedrock with many joints, fissures, and pores can absorb rainwater, especially after long-term weathering (Xiong et al., 2012), and b) bedrock has interception and gathering effects, reducing the velocity of surface runoff (Kheir et al., 2008; Wang et al., 2010b). Dai et al. (2017) studied the relationship between soil erosion and the bedrock bareness rate in a karst area using artificial rainfall simulation tests to simulate the dual hydrological structure with surface bed rock bareness and underground pore fissures (Fig. S2). They found that the coefficient of association ( $R$ ) between surface sediment and the bedrock bareness rate was  $-0.076$  ( $p < 0.01$ ). Based on this result, we modified the RUSLE model to simulate karst soil erosion using the coefficient of determination ( $R^2$ ), which measured how well soil erosion might be constructed from bedrock bareness. Therefore, Eq. (1) can be modified as follows:

$$A = (1 - 0.076^2 \times a) \times R \times K \times LS \times C \times P \quad (2)$$

where  $a$  is a correctional coefficient. The data were acquired from mean

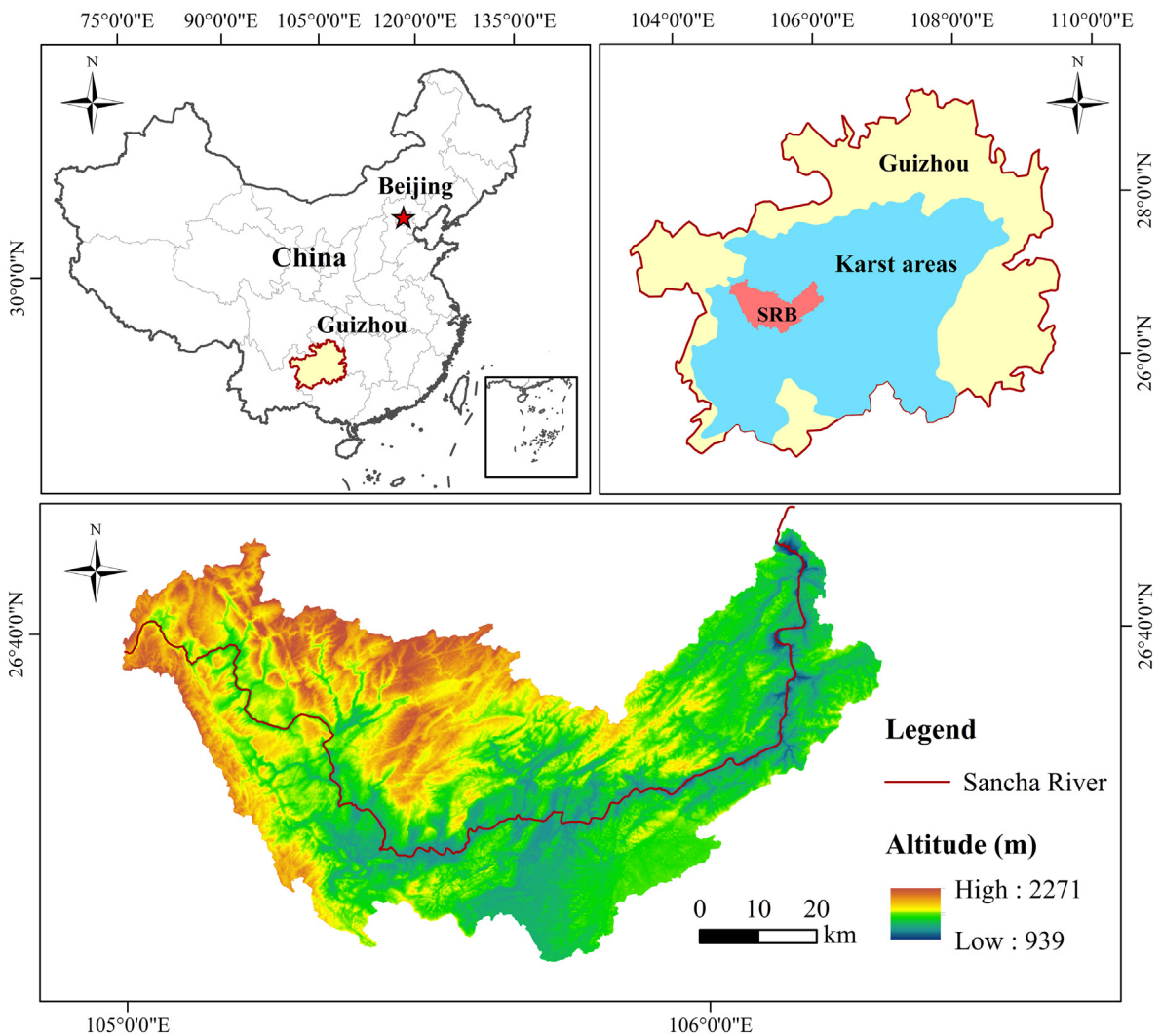


Fig. 1. The location of the study area in Guizhou Province, China (upper), and the regional topography (lower).

**Table 1**  
Correctional coefficient for different degrees of rocky desertification.

Rocky desertification	None	Potential	Light	Moderate	High	Severe
Bedrock bareness rate (%)	< 20	20–30	31–50	51–70	71–90	> 90
<i>a</i>	10	25	40	60	80	95

bedrock bareness rates for different levels of rocky desertification (Table 1). Karst soil erosion with lithology types of carbonate rocks was simulated using Eq. (2), and non-karst soil erosion with lithology types of non-carbonate rocks was simulated using Eq. (1). Clastic rock was the only non-carbonate rock type in the study area, therefore, we used the unmodified RUSLE model to simulate soil erosion in areas where there were distributions of clastic rock. In areas where carbonate rocks were presented, the modified RUSLE model was applied. The distribution of carbonate and non-carbonate areas is shown in Fig. S1a. To differentiate soil erosion in karst and non-karst areas, the term “karst soil erosion” was used to represent soil erosion in karst areas.

The *R* factor was computed using average annual rainfall data, and the following equations (Renard and Freimund, 1994):

$$R = 0.04830P^{1.610} (P < 850 \text{ mm}) \tag{3}$$

$$R = 587.8 - 1.219P + 0.004105P^2 (P > 850 \text{ mm}) \tag{4}$$

where *P* (mm) is the average annual rainfall, calculated using the sliding average method with three years of data.

*K* was simulated using the erosion-productivity impact calculator model proposed by Williams et al. (1989).

*L* and *S* were calculated based on the interaction of topography and flow accumulation. Due to the discontinuous nature of karst surface runoff, the accuracy of the *L* factor is closely related to the accumulated area threshold and resolution of the DEM (Feng et al., 2016). Thus, 9-m DEM data were used in this study. The *L* factor was computed using the method developed by Zhang et al. (2013), based on the expression in McCool et al. (1989). The *S* factor was generated as follows, based on McCool et al. (1987):

$$L = \left( \frac{\lambda}{22.13} \right)^\alpha \tag{5}$$

$$\alpha = \left( \frac{\beta}{\beta + 1} \right) \tag{6}$$

$$\beta = \frac{\sin \theta}{3 \times (\sin \theta)^{0.8} + 0.56} \tag{7}$$

$$S = 10.8 \times \sin \theta + 0.03 (\theta < 9\%, \lambda > 4.6 \text{ m}) \tag{8}$$

$$S = 16.8 \times \sin \theta - 0.50 (\theta \geq 9\%, \lambda > 4.6 \text{ m}) \tag{9}$$

$$S = 3.0 \times (\sin \theta)^{0.8} + 0.56 (\lambda < 4.6 \text{ m}) \tag{10}$$

**Table 2**  
The *C* and *P* values.

Land use	Paddy land	Dry land	Forest	Open forest	Shrub	Grassland	Water body	Construction land	Bare rock
<i>C</i>	0.1	0.22	0.006	0.01	0.01	0.04	0	0	0
<i>P</i>	0.15	0.4	1	1	1	1	0	0	0

where  $\lambda$  is slope length,  $\alpha$  is a variable slope length exponent,  $\beta$  is a factor related to the slope value, and  $\theta$  is the slope value.

The factors *C* and *P* (Table 2) were acquired from previous studies of karst areas in southwest China (Feng et al., 2016; Xu et al., 2010; Zeng et al., 2017).

The data used in this study, had to be scaled and transformed for uniformity due to the diversity of the sources used. All data were transformed to the Albers\_Conic\_Equal\_Area projection. The *LS* factor was scaled up from a 9-m resolution to a 30-m resolution. Since rainfall data varied little within a 1-km area on an annual scale, it was feasible to transform the resolution of the *R* factor from 1 km to 30 m. Furthermore, the soil type data had low spatial heterogeneity; thus it was reasonable to scale the *K* factor down to a resolution of 30 m from a 1-km resolution. The grid nesting method used is described in Fig. S3.

### 2.3.2. Geographical detector method

The geographical detector method is a spatial variance analysis method developed to detect the spatial heterogeneity of an event and assess the relationship between the event and potential risk factors, including environmental and anthropogenic factors (Wang et al., 2010a). It contains four formulas, a factor detector, an interaction detector, a risk detector, and an ecological detector.

The basis of the method is that if the sum of the variance of the sub-areas in a region is less than the variance of the total region, spatial heterogeneity exists in the area (Wang and Xu, 2017). Assume that *X* is an influencing factor and *Y* is an event. The underlying assumption of the geographical detector method is that, if the *X* factor is associated with *Y*, then the spatial distribution of *Y* is similar to that of *X* (Luo et al., 2016). Under perfect conditions, if *X* completely controls the distribution of *Y*, the sum of the variance within all the zones would be zero. The proportion of the spatial distribution of *Y* that can be explained by *X* is measured by the power of determinant (*q* value). The calculation is as follows:

$$q = 1 - \frac{1}{N\sigma^2} \sum_{z=1}^L N_z \sigma_z^2 \tag{11}$$

$$\sigma_z^2 = \frac{1}{N_z - 1} \sum_{i=1}^{N_z} (Y_{z,i} - \bar{Y}_z)^2 \tag{12}$$

$$\sigma^2 = \frac{1}{N - 1} \sum_{j=1}^N (Y_j - \bar{Y})^2 \tag{13}$$

where  $\sigma^2$  is the variance of *Y* in the region,  $\sigma_z^2$  is the variance in zone *Z* divided by *X*, *N* is the number of sample units in the region, *N<sub>z</sub>* is the number of sample units in zone *Z*, and *L* is the number of zones. *Y<sub>z,i</sub>* and *Y<sub>j</sub>* are the values of *Y* in the *i*th sample unit of zone *Z* and the *j*th sample unit of the entire region respectively.

The *q* value of the interaction between two influencing factors was calculated using the interaction detector module, which detects whether the factors interact or lead to soil erosion independently by comparing *q<sub>X1∩X2</sub>* with the values of *q<sub>X1</sub>* and *q<sub>X2</sub>*. If *q<sub>X1∩X2</sub>* > *q<sub>X1</sub>*, and *q<sub>X2</sub>*, the factors enhance each other, if *q<sub>X1∩X2</sub>* < *q<sub>X1</sub>* or *q<sub>X2</sub>*, the factors weaken each other, and if *q<sub>X1∩X2</sub>* = *q<sub>X1</sub>* + *q<sub>X2</sub>*, the factors are independent. The risk detector can determine the area with the highest susceptibility to soil erosion.

The input data for the geographical detector must be categorical layers (e.g., land use type, lithology, and geomorphology). Continuous datasets (e.g., rainfall, slope, and elevation) must be categorized. In this study, we divided rainfall, slope, and elevation into nine strata using

the natural break method.

## 3. Results and analysis

### 3.1. Model validation and spatial distribution of soil erosion

The modified RUSLE model was used to calculate soil erosion rates from 1980 to 2015 in the karst areas, and the unmodified RUSLE model was used in the non-karst areas. The validation of the model was based on two aspects: the value of soil erosion and its trend at a large scale (basin or region scale), and the spatial distribution of soil erosion in areas of different degrees of rocky desertification. Due to that with spatially downscaling and upscaling, the spatial heterogeneity will change and the predominant processes may be different, details regarding erosion characteristics that were ignored at a large scale will show up at a small scale, and the macro law presented at larger scales may disappear in smaller scales (Li and Cai, 2005). Thus, the soil erosion conditions at small scales (such as runoff plot experiments) were not applied in the section on model validation.

The average annual soil erosion in the SRB during the 1980s, 1990s, and 2000s (Fig. 2) was 15.41, 15.30, and 14.04 t ha<sup>-1</sup> a<sup>-1</sup>, respectively, presenting a slightly decreasing trend. Despite this, the rate of soil erosion remained much higher than the soil loss tolerance and soil formation rate (Bai and Wang, 2011; Li et al., 2006; Zhang et al., 2010). Data from the water and soil conservation monitoring station in Guizhou Province showed that average soil erosion decreased there, from 14.32 t ha<sup>-1</sup> a<sup>-1</sup> in the 1990s to 13.61 t ha<sup>-1</sup> a<sup>-1</sup> in the 2000s. Other studies (Feng et al., 2016; Xu et al., 2008; Zeng et al., 2017) have found that soil erosion ranged from 14.4 to 28.7 t ha<sup>-1</sup> a<sup>-1</sup> in karst basins in southwest China. These results were consistent with those of this study.

Using the unmodified RUSLE model, the calculated karst soil erosion rates for the 2000s in moderate, high, and severe rocky desertification areas were 14.67 t ha<sup>-1</sup> a<sup>-1</sup>, 18.32 t ha<sup>-1</sup> a<sup>-1</sup> and 16.37 t ha<sup>-1</sup> a<sup>-1</sup> respectively (Fig. S4). From moderate to high rocky desertification areas and from moderate to severe rocky desertification areas, soil erosion increased by 3.65 t ha<sup>-1</sup> a<sup>-1</sup> and 1.70 t ha<sup>-1</sup> a<sup>-1</sup>, representing increases of 24.9% and 11.6%, respectively. However, in areas with severe rocky desertification, the surface soil layer is too shallow to induce substantial levels of soil erosion. After modifying the model, soil erosion generally displayed a decreasing trend as rocky desertification increased (Fig. S4). This was consistent with a previous study (Zeng et al., 2017), which found that soil erosion decreased as rocky desertification worsened. After modification, the calculated soil erosion in areas with moderate, high and severe rocky desertification was 9.55 t ha<sup>-1</sup> a<sup>-1</sup>, 9.91 t ha<sup>-1</sup> a<sup>-1</sup>, and 7.38 t ha<sup>-1</sup> a<sup>-1</sup>, respectively. From areas of moderate to high rocky desertification, soil erosion increased by 3.8%. In addition, soil erosion in areas with severe rocky desertification decreased by 22.7% compared to that in areas of moderate rocky desertification.

About half the study area experienced light soil erosion, followed by slight and medium soil erosion, and the sum of the areas of high and very high erosion accounted for < 2% of the total area in the 2000s (Table S2). Although only 13.68% of the study area experienced medium soil erosion, it accounted for 32.10% of total soil loss. Similarly, only 1.85% of the area experienced high soil erosion; however, this area, was responsible for 7.47% of the total soil loss. Mean soil erosion in karst areas with a value of 13.69 t ha<sup>-1</sup> a<sup>-1</sup> (Fig. S5a)

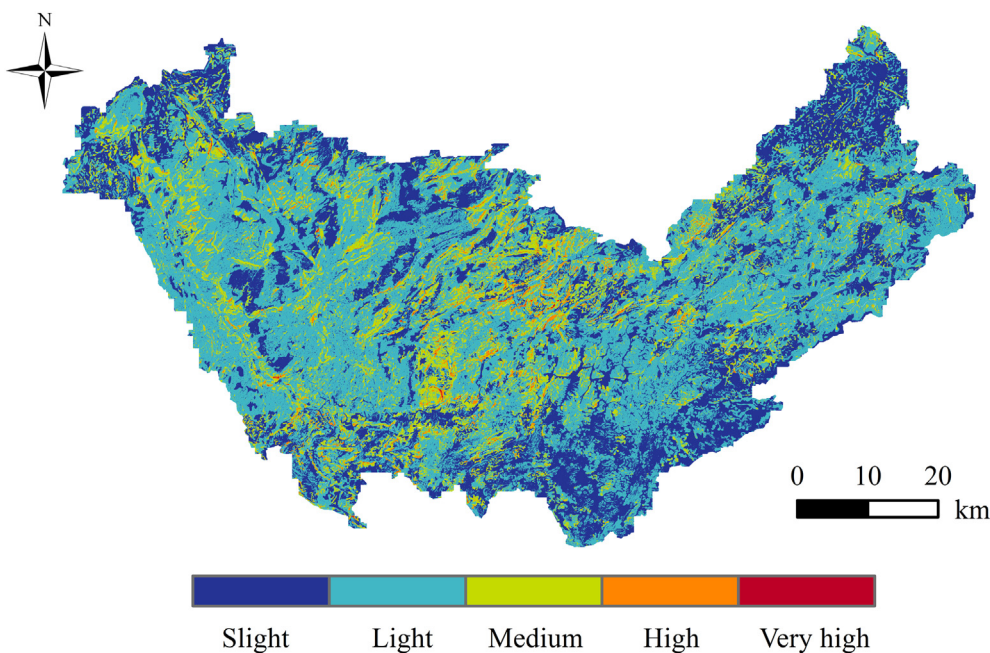


Fig. 2. Degree of soil erosion in the 2000s.

was lower than that in non-karst areas; the value in the latter was  $17.43 \text{ t ha}^{-1} \text{ a}^{-1}$  (Fig. S5b). About 85.3% of the karst areas experienced by slight and light soil erosion, 75.3% of the non-karst areas were occupied by slight and light soil erosion. And 1.65% of the karst areas suffered from high and very high soil erosion, 4.77% of the non-karst areas suffered from high and very high soil erosion.

3.2. Quantitative attribution analysis of soil erosion

3.2.1. Temporal analysis of the determinants of soil erosion

In karst areas, in the 1980s, 1990s, and 2000s, the influencing factors, arranged from highest to lowest  $q$ -value, were: land use, slope, elevation, rainfall, lithology, and geomorphology (Table S3). The interaction module results indicated that the enhancement between land use type and slope, land use type and rainfall, and rainfall and slope were the most significant interactions, and the  $q$  values of these combinations were higher than the sum of the single factors. Fig. 3 shows the  $q$  values of the influencing factors and the combinations of rainfall, slope, and land use in seven typical years (1980, 1990, 1995, 2000, 2005, 2010, and 2015).

The  $q$  value of land use increased, the  $q$  values of slope and rainfall slightly decreased, and the remaining factors remained nearly unchanged (Fig. 3a). The  $q$  values of the interactions of rainfall and land use, and slope and land use were relatively stable. The combination of slope and land use, which had the highest  $q$  value, predominantly explained the spatial heterogeneity of soil erosion, followed by land use and rainfall, and rainfall and slope (Fig. 3b). In non-karst areas, the  $q$  value of land use was lower than that in karst areas, and it was still the dominant factor of soil erosion distribution, followed by slope; however the influence of geomorphology on soil erosion was not significant in most years (Fig. S6).

To determine which land use type was most closely related to karst soil erosion, we calculated the area of dry land, forest, construction land, dry land with slopes of  $10\text{--}15^\circ$ , and dry land with slope  $> 15^\circ$  during the seven typical years. A partial correlation analysis between the areas of these land use types and karst soil erosion was conducted. The partial correlation coefficient of dry land with slope  $> 15^\circ$  and karst soil erosion reached 0.91, which was the only factor that passed the significance test ( $p < 0.1$ ). Thus, steeply sloping cropland was the

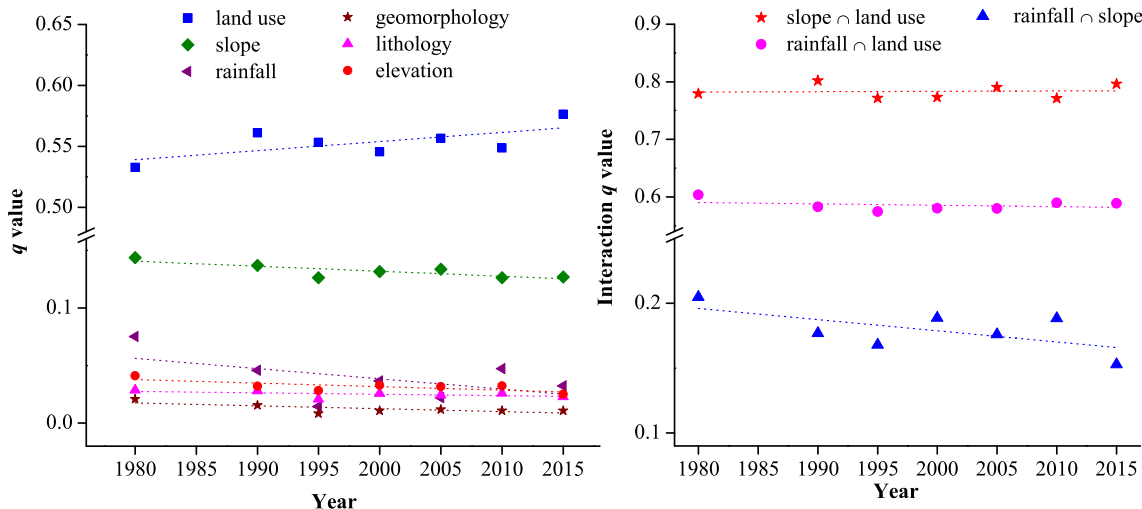


Fig. 3. The (a)  $q$  values and (b) interaction  $q$  values of influencing factors on karst soil erosion distribution.

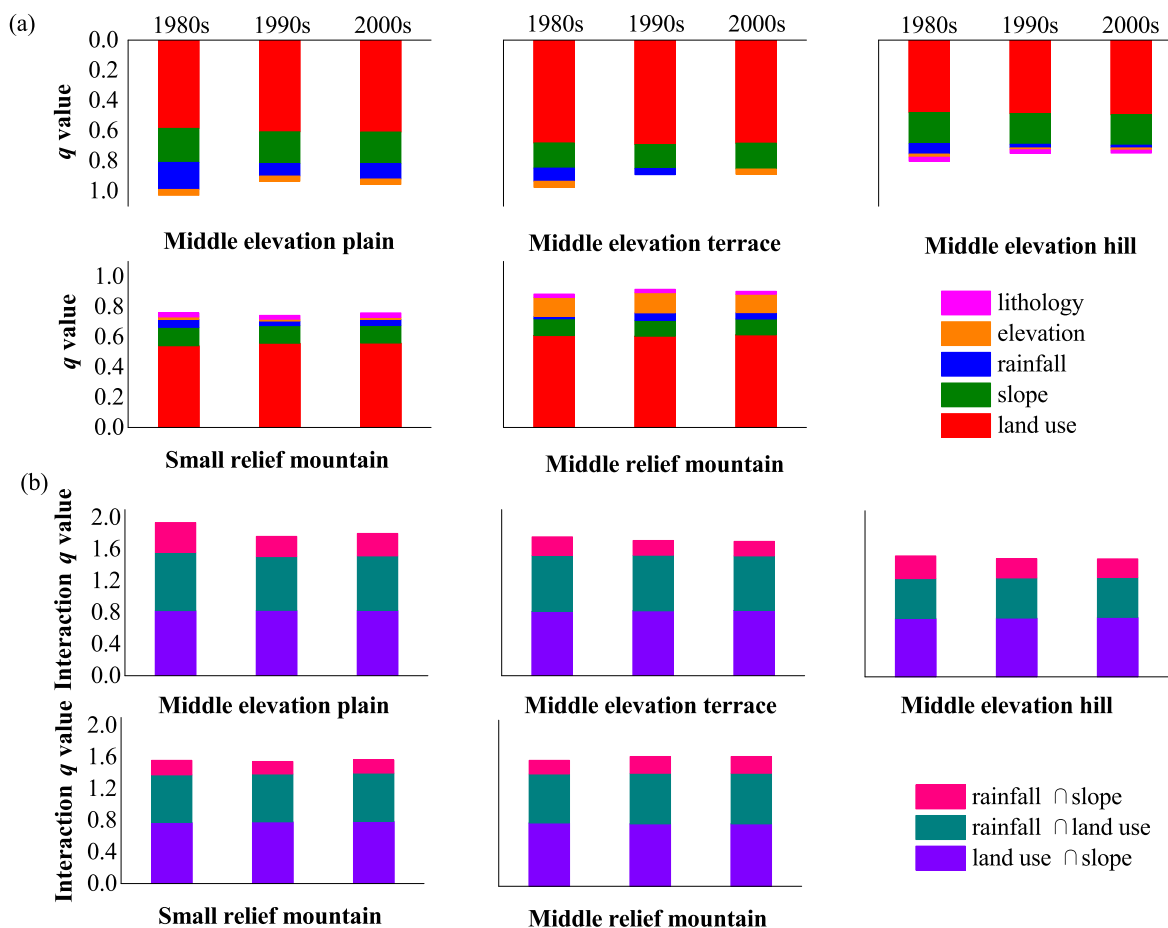


Fig. 4. The *q* values of (a) influencing factors and (b) their combinations for different karst geomorphological types during the past three decades.

land use type most susceptible to soil erosion.

### 3.2.2. Regional differentiation based on diverse karst geomorphological types

Karst environmental factors are characterized by high spatial heterogeneity. Thus, a geographical detector method was applied to five geomorphological types to detect the dominant factors for karst soil erosion in each geomorphological type. Generally, there were no significant difference in the *q* values of single factors or their combinations in any given geomorphological type during the three periods, but the *q* values varied among the different geomorphological types (Fig. 4). The *q* value of rainfall in the middle elevation plain was much higher than that in the other geomorphological types (Fig. 4a), due to the small differences in relief and low proportion of steep sloped dry land in the region (Table S1, 4), in which slight changes in rainfall can trigger significant soil erosion. In mountainous areas, middle elevation hill had a larger *q* value of slope than small relief mountain, which had a larger *q* value than middle relief mountain. Thus, we inferred that in mountainous areas with complex climate and anthropogenic activities, the *q* value of the slope decreased with the increasing relief. At 0.12, the *q* value of the elevation of middle relief mountain was much higher compared to the other types. The influence of lithology on soil erosion distribution was not significant in middle elevation plain and middle elevation terrace.

The *q* value of the interaction between land use and rainfall was highest in middle elevation plain, followed by middle elevation terrace (Fig. 4b). This was because slopes and reliefs are lower in relatively flat areas than in mountainous areas (Table S1, 4), and the interaction of land use and rainfall can better explain soil erosion distribution. The high-risk area (95% confidence level) of karst soil erosion differed

among the geomorphological types (Table S5). In mountainous areas, regions with slopes > 38° were most sensitive to severe soil erosion. In relatively flat areas, slopes of 16–20° in middle elevation plain and middle elevation terrace were at the greatest risk of erosion. Of the land use types, dry land was at the greatest risk of karst soil erosion.

### 3.3. Quantitative attribution analysis of karst soil erosion variability

#### 3.3.1. Temporal dynamic characteristics of karst soil erosion determinants

During the past 36 years, karst soil erosion showed fluctuating trends that correlated well with the average annual rainfall change (Fig. 5). The correlation coefficient between soil erosion and precipitation was 0.996 ( $p < 0.01$ ). In general, soil erosion displayed a decreasing trend ( $p < 0.01$ ). Karst soil erosion decreased in the 1980s, increased in the 1990s, and then declined again in the 2000s. Fig. S7 presented the spatial distribution of karst soil erosion variability in the three periods.

Karst soil erosion variability differed among the periods. The major driving factors of soil erosion, including land use change, rainfall variability, and their interactions with slope, were chosen to analyze soil erosion variability. The average karst soil erosion variability was lower in the whole period than in the three decades (Table S6), and land use change was the dominant influencing factor (Table 3). Although the *q* value of land use change decreased over the three periods, it was the dominant factor in the 1980s and 1990s, and land use change and slope was the dominant interaction in those decades. Soil erosion variability was negative in most areas in the 1980s, with low spatial heterogeneity (Fig. S7a), and 54% of the variability distribution could be explained by land use change (Table 3). In the 1990s, soil erosion variability was mostly positive (Fig. S7b), and land use change was the

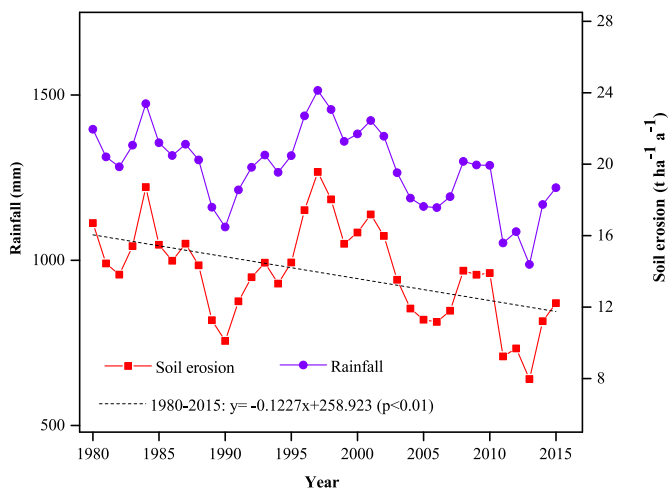


Fig. 5. Karst soil erosion and rainfall variation (1980–2015).

**Table 3**  
The *q* values of the influencing factors and their combinations (1980–2015).

	Land use change	Rainfall variability	Land use change ∩ slope	Land use change ∩ rainfall	Rainfall ∩ slope
1980s	0.54	0.07	0.69	0.67	0.11
1990s	0.10	0.05	0.23	0.16	0.20
2000s	0.07	0.19	0.19	0.27	0.30
1980–2015	0.28	0.09	0.40	0.38	0.18

dominant influencing factor, which was responsible for 10% of the variability distribution. In the 2000s, rainfall variability and the combination of rainfall with slope were the dominant single and interaction factors driving the negative variability of soil erosion. The *q* value of the interaction between land use change and slope decreased, while the interaction between rainfall and slope increased over the three decades.

### 3.3.2. Regional differentiation for diverse karst geomorphological types

The karst soil erosion variability and dominant driving factor varied among different geomorphological types. Soil erosion variability was lower in relatively flat areas than in mountainous areas (Table S6). In the 1980s, the dominant driving factor of soil erosion variability in the five geomorphological types was land use change, with *q* values higher than 0.53 (Fig. 6). The *q* values of rainfall variability were small, indicating that the karst soil erosion variability distribution was mainly explained by land use change. The dominant interaction was between land use change and slope, with a combined *q* value higher than 0.65 (Fig. 6). In the 1990s, the dominant driving factor was rainfall variability in middle elevation plain, and land use change in the other geomorphological types. In the 2000s, the dominant influencing factor was rainfall variability across all geomorphological types.

## 4. Discussion

Soil erosion methods and indicators applied to non-karst areas generally cannot reflect the conditions in karst areas (Zeng et al., 2017). In karst areas, thin soil with a slow soil formation rate makes a poor habitat for plants, resulting in fragile ecosystems where soil erosion occurs readily. Moreover, karst areas located in humid climate zones may experience severe soil erosion during frequent heavy rainfall, generating rocky desertification causing discontinuous runoff that can reduce the effects of slope length (Feng et al., 2016). In this study, we optimized the RUSLE model for areas of carbonate rocks based on the relationship between soil erosion and bedrock bareness rates (Dai et al., 2017), and 9-m DEM data were applied to improve the simulation

accuracy of the *L* factor.

### 4.1. Soil erosion characteristics in karst area

#### 4.1.1. Influencing factors of karst soil erosion

The soil erosion distribution in karst areas depends on both anthropogenic activities and natural conditions. Peng and Wang (2012) found that soil loss was related to land use and rainfall regimes on karst hillslopes. Meanwhile, Xu and Shao (2006) demonstrated that dry land with slopes of 6–25° should be managed to prevent soil erosion. However, none of these studies quantified the influence of factors (or combinations of factors) contributing to soil erosion. The present study confirmed that land use type, slope, rainfall, elevation, lithology, and geomorphology had significant impacts on karst soil erosion. Land use predominantly explained the spatial heterogeneity of karst soil erosion. Its *q* value displayed an increasing trend over the past 36 years, indicating a rising influence of anthropogenic activities on soil erosion, which predominantly included activities related to land use management policies, such as the “Grain for Green” project. Among the different geomorphological types, the dominant influencing factor was land use type, followed by slope. However, the *q* values of the influencing factors and the high-risk areas of karst soil erosion differed substantially. These differences were determined by the local characteristics of each geomorphological type. For example, the *q* value of elevation in middle elevation mountain was higher than that of other areas, because the relative elevation was higher (Table S4). Elevation can reflect differences in climate and topography associated with middle elevation mountains. These results indicate that differences in karst soil erosion characteristics among diverse geomorphological types should be considered during soil erosion control and management.

#### 4.1.2. Temporal characteristics of karst soil erosion

Understanding the long-term soil erosion dynamic characteristics provides a foundation to clarify the driving mechanism behind soil erosion change, and further provides reference for researchers and policy makers to formulate solutions and regulations to prevent soil erosion. In karst areas, under the background of climate change and ecological restoration, climate conditions and land use/cover circumstances vary temporally, driving changes in soil erosion. In this study, land use change was the dominant driving factor of karst soil erosion variability over the past 36 years. During the three study periods, land use change was dominant in the 1980s with a large area of land use change (3.82% of the carbonate area) and small rainfall variability (−12.53 mm). In the 1990s, land use change, with a *q* value of 0.1, dominated the positive soil erosion variability, with a large area of land use change (3.75% of the carbonate area) and high rainfall variability (33.94 mm). In the 2000s, rainfall variability dominated, with a small area of land use change (1.24% of the carbonate area) and moderate rainfall variability (−17.97 mm). Thus, we confirmed that in different periods, the dominant driving factor was affected by the characteristics of land use change and climate change. Over the entire study period, karst soil erosion variability was lower compared to the 10-year time scale, and rainfall and karst soil erosion showed consistent trends (*p* < 0.01), with the fluctuation in soil erosion rates affected by rainfall variation.

### 4.2. Uncertainty analysis and future perspectives

In this study, we modified the RUSLE model to improve the simulation accuracy for karst environments. On the one hand, the correlation between soil erosion and bedrock bareness was applied to solve the issues of bedrock resistance to soil erosion and less erodible soil in areas with severe rocky desertification; on the other hand, high-resolution topography data were used to mitigate the impact of bedrock on slope length. However, some limitations remain and require further study. First, the correlation coefficient of karst soil erosion and bedrock

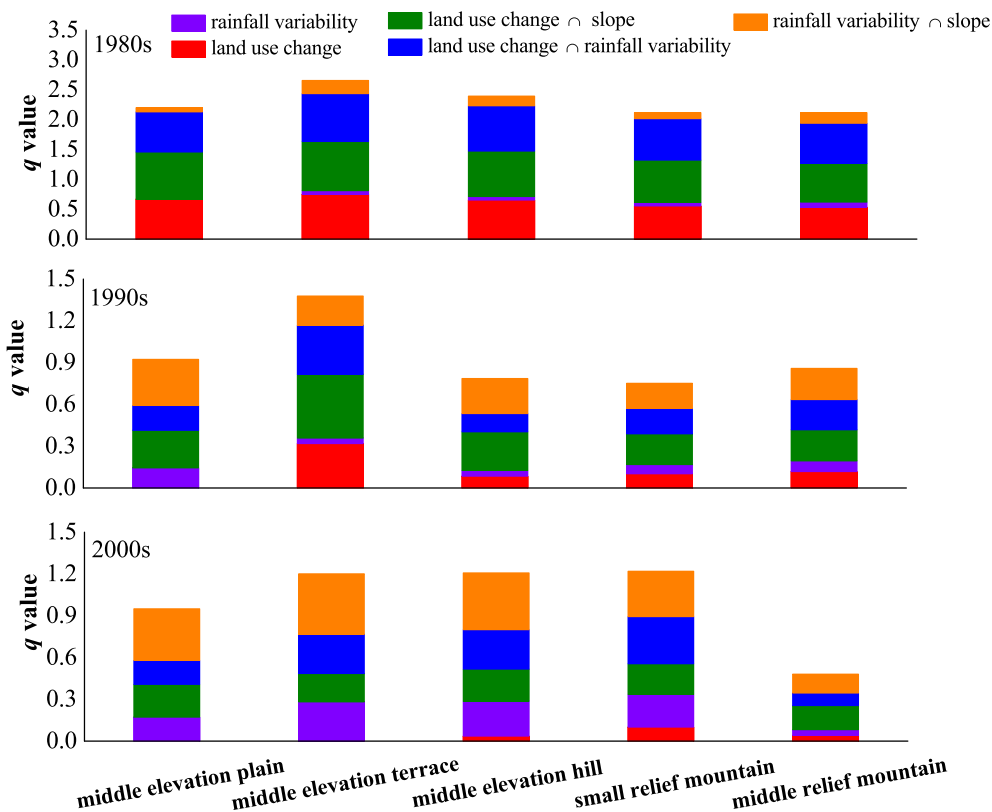


Fig. 6. The *q* values of the driving factors and their interactions on karst soil erosion variability for different geomorphological types (1980s, 1990s, and 2000s).

bareness rate was acquired with artificial rainfall simulation tests, which differed from real conditions. Hence, future studies should assess these factors in field experiments. Second, the process of soil erosion in karst areas is complex, and this study only considered the surface conditions; future work should also consider underground soil erosion processes.

### 5. Conclusion

The current study identified the dominant factors (and combination factors) of karst soil erosion and its variability over the past 36 years, based on the modified RUSLE model and the geographical detector method. The strength of association between the factors and karst soil erosion differed temporally and across different geomorphological types.

Land use was the dominant factor influencing the karst soil erosion distribution in the SRB, located in southwest China. The interactions between two influencing factors can enhance their impacts on karst soil erosion, and the combination of land use and slope was the dominant interaction factor affecting soil erosion. Karst soil erosion in the SRB exhibited a decreasing trend overall, while the influence of anthropogenic activities increased over time. The strength of association between the influencing factors and karst soil erosion differed among the geomorphological types. For example, in mountainous areas, the *q* value of slope decreased with increasing relief.

The dominant driving factors and their *q* values of karst soil erosion variability were affected by land use change and climate change across the whole period. Land use change dominated in the 1980s and 1990s. Rainfall variability dominated in the 2000s. In addition, in relatively flat areas, mean value of karst soil erosion variability was lower than in mountainous areas.

Karst soil erosion management and control remains a challenging task. This study confirmed that controlling karst soil erosion based on different geomorphological types and prohibiting steep cropland with

slopes higher than 15° are optimal policy choices in karst areas.

### Funding

This work was supported by the National Natural Science Foundation of China [grant number 41671098], the National Basic Research Program of China [grant number 2015CB452702] and the ‘Strategic Priority Research Program’ of the Chinese Academy of Sciences (grant numbers XDA20020202, XDA19040304).

### Appendix A. Supplementary data

Supplementary data to this article can be found online at <https://doi.org/10.1016/j.catena.2018.08.035>.

### References

Bai, X.Y., Wang, S.J., 2011. Relationships between soil loss tolerance and karst rocky desertification. *J. Nat. Resour.* 26 (8), 1315–1322 (in Chinese).  
 Bai, X.Y., Zhang, X.B., Long, Y., Liu, X.M., Zhang, S.Y., 2013. Use of <sup>137</sup>Cs and <sup>210</sup>Pbex measurements on deposits in a karst depression to study the erosional response of a small karst catchment in Southwest China to land-use change. *Hydrol. Process.* 27 (6), 822–829.  
 Boix-Fayos, C., Martinez-Mena, M., Arnau-Rosalen, E., Calvo-Cases, A., Castillo, V., Albaladejo, J., 2006. Measuring soil erosion by field plots: understanding the sources of variation. *Earth Sci. Rev.* 78 (3–4), 267–285.  
 Borrelli, P., Panagos, P., Maerker, M., Modugno, S., Schuett, B., 2017. Assessment of the impacts of clear-cutting on soil loss by water erosion in Italian forests: first comprehensive monitoring and modelling approach. *Catena* 149, 770–781.  
 Campbell, I.A., 1992. Spatial and temporal variations in erosion and sediment yield. In: *Erosion and Sediment Transport Monitoring Programmes in River Basins*. 210. pp. 455–465.  
 Chen, H., Oguchi, T., Wu, P., 2017. Assessment for soil loss by using a scheme of alternative sub-models based on the RUSLE in a Karst Basin of Southwest China. *J. Integr. Agric.* 16 (2), 377–388.  
 Dai, Q.H., Peng, X.D., Yang, Z., Zhao, L.S., 2017. Runoff and erosion processes on bare slopes in the karst rocky desertification area. *Catena* 152, 218–226.  
 Febles-Gonzalez, J.M., Vega-Carreño, M.B., Tolon-Becerra, A., Lastra-Bravo, X., 2012. Assessment of soil erosion in karst regions of Havana, Cuba. *Land Degrad. Dev.* 23

- (5), 465–474.
- Feng, T., Chen, H.S., Polyakov, V.O., Wang, K.L., Zhang, X.B., Zhang, W., 2016. Soil erosion rates in two karst peak-cluster depression basins of northwest Guangxi, China: comparison of the RUSLE model with  $^{137}\text{Cs}$  measurements. *Geomorphology* 253, 217–224.
- Guo, Q.K., Hao, Y.F., Liu, B.Y., 2015. Rates of soil erosion in China: a study based on runoff plot data. *Catena* 124, 68–76.
- Hutchinson, M.F., 2001. Anusplin Version 4.2 User Guide. FSES, Canberra, ACT.
- Irvem, A., Topaloglu, F., Uygur, V., 2007. Estimating spatial distribution of soil loss over Seyhan River Basin in Turkey. *J. Hydrol.* 336 (1–2), 30–37.
- Kefi, M., Yoshino, K., Setiawan, Y., Zayani, K., Boufaroua, M., 2011. Assessment of the effects of vegetation on soil erosion risk by water: a case of study of the Batta watershed in Tunisia. *Environ. Earth Sci.* 64 (3), 707–719.
- Kheir, R.B., Abdallah, C., Khawlie, A., 2008. Assessing soil erosion in Mediterranean karst landscapes of Lebanon using remote sensing and GIS. *Eng. Geol.* 99 (3–4), 239–254.
- Kim, J., Ivanov, V.Y., Faticchi, S., 2016. Environmental stochasticity controls soil erosion variability. *Sci. Rep.* 6.
- Li, S.C., Cai, Y.L., 2005. Some scaling issues of geography. *Geogr. Res.* 24 (1), 11–18 (in Chinese).
- Li, Y.B., Wang, S.J., Wei, C.F., Luo, G.J., 2006. The spatial distribution of soil loss tolerance in carbonate area in Guizhou province. *Earth Environ. Sci.* 34 (4), 36–40 (in Chinese).
- Li, Y., Bai, X.Y., Zhou, Y.C., Qin, L.Y., Tian, X., Tian, Y.C., Li, P.L., 2016. Spatial-temporal evolution of soil erosion in a typical mountainous karst basin in SW China, based on GIS and RUSLE. *Arab. J. Sci. Eng.* 41 (1), 209–221.
- Luo, W., Jasiewicz, J., Stepinski, T., Wang, J.F., Xu, C.D., Cang, X.Z., 2016. Spatial association between dissection density and environmental factors over the entire conterminous United States. *Geophys. Res. Lett.* 43 (2), 692–700.
- Martinez-Casasnovas, J.A., Ramos, M.C., Benites, G., 2016. Soil and water assessment tool soil loss simulation at the sub-basin scale in the Alt Penedes-Anoia Vineyard Region (Ne Spain) in the 2000s. *Land Degrad. Dev.* 27 (2), 160–170.
- McCool, D.K., Brown, L.C., Foster, G.R., Mutchler, C.K., Meyer, L.D., 1987. Revised slope steepness factor for the universal soil loss equation. *Trans. ASAE* 30 (5), 1387–1396.
- McCool, D.K., Foster, G.R., Mutchler, C.K., Meyer, L.D., 1989. Revised slope length factor for the universal soil loss equation. *Trans. ASAE* 32 (5), 1571–1576.
- Ouyang, W., Skidmore, A.K., Hao, F.H., Wang, T.J., 2010. Soil erosion dynamics response to landscape pattern. *Sci. Total Environ.* 408 (6), 1358–1366.
- Peng, T., Wang, S.J., 2012. Effects of land use, land cover and rainfall regimes on the surface runoff and soil loss on karst slopes in southwest China. *Catena* 90, 53–62.
- Renard, K.G., Freimund, J.R., 1994. Using monthly precipitation data to estimate the R-factor in the revised USLE. *J. Hydrol.* 157 (1–4), 287–306.
- Renard, K.G., Foster, G.R., Weesies, G.A., McCool, D.K., Yoder, D.C., 1997. Predicting soil erosion by water: a guide to conservation planning with the revised universal soil loss equation (RUSLE). In: *Agriculture Handbook*. USDA, Washington, DC.
- Sun, W.Y., Shao, Q.Q., Liu, J.Y., 2013. Soil erosion and its response to the changes of precipitation and vegetation cover on the Loess Plateau. *J. Geogr. Sci.* 23 (6), 1091–1106.
- Tian, Y.C., Wang, S.J., Bai, X.Y., Luo, G.J., Xu, Y., 2016. Trade-offs among ecosystem services in a typical karst watershed, SW China. *Sci. Total Environ.* 566, 1297–1308.
- Vanacker, V., Govers, G., Barros, S., Poesen, J., Deckers, J., 2003. The effect of short-term socio-economic and demographic change on landuse dynamics and its corresponding geomorphic response with relation to water erosion in a tropical mountainous catchment, Ecuador. *Landsc. Ecol.* 18 (1), 1–15.
- Wang, S.J., 2003. The most serious eco-geologically environmental problem in southwestern China karst rocky desertification. *Bull. Mineral. Petrol. Geochem.* 22 (2), 120–126 (in Chinese).
- Wang, J.F., Xu, C.D., 2017. Geodetector: principle and prospective. *Acta Geograph. Sin.* 72 (1), 116–134 (in Chinese).
- Wang, S.J., Liu, Q.M., Zhang, D.F., 2004. Karst rocky desertification in southwestern China: geomorphology, landuse, impact and rehabilitation. *Land Degrad. Dev.* 15 (2), 115–121.
- Wang, J.F., Li, X.H., Christakos, G., Liao, Y.L., Zhang, T., Gu, X., Zheng, X.Y., 2010a. Geographical detectors-based health risk assessment and its application in the neural tube defects study of the Heshun Region, China. *Int. J. Geogr. Inf. Sci.* 24 (1), 107–127.
- Wang, J., Cai, X.F., Lei, L., Zhang, H., 2010b. Laboratory simulation on soil erosion under different bedrock outcrop rate in Southwest karst area, China. *Carsologica Sinica* 29 (1), 1–5.
- Williams, J.R., Jones, C.A., Kiniry, J.R., Spanel, D.A., 1989. The EPIC crop growth-model. *Trans. ASAE* 32 (2), 497–511.
- Wischmeier, W., Smith, D., 1978. *Predicting Rainfall Erosion Losses: A Guide to Conservation Planning (Agriculture Handbook)*. USDA, Washington, DC.
- Xiong, K.N., Li, J., Long, M.Z., 2012. Features of soil and water loss and key issues in demonstration areas for combating karst rocky desertification. *Acta Geograph. Sin.* 67 (7), 878–888 (in Chinese).
- Xu, Y., Long, J., 2005. Effect of soil physical properties on soil erosion in Guizhou karst mountainous region. *J. Soil Water Conserv.* 19 (1), 157–159, 175 (in Chinese).
- Xu, Y.Q., Peng, J., 2008. Effects of simulated land use change on soil erosion in the Maotiao River Watershed of Guizhou province. *Lett. Spat. Resour. Sci.* 30 (8), 1218–1225 (in Chinese).
- Xu, Y.Q., Shao, X.M., 2006. Estimation of soil erosion supported by GIS and RUSLE: a case study of Maotiaohe Watershed, Guizhou Province. *J. Beijing For. Univ.* 28 (4), 67–71 (in Chinese).
- Xu, Y.Q., Shao, X.M., Kong, X.B., Peng, J., Cai, Y.L., 2008. Adapting the RUSLE and GIS to model soil erosion risk in a mountains karst watershed, Guizhou Province, China. *Environ. Monit. Assess.* 141 (1–3), 275–286.
- Xu, Y.Q., Huang, J., Feng, Y., Zhou, D., 2010. Soil erosion economic loss under different land use structures: a case study of Maotiao River Watershed, Guizhou Province. *Prog. Geogr.* 29 (11), 1451–1456 (in Chinese).
- Yan, Y.J., Dai, Q.H., Fu, W.B., Peng, X.D., Jin, L., 2017. Runoff and sediment production processes on a karst bare slope. *Acta Ecol. Sin.* 37 (6), 2067–2079 (in Chinese).
- Yao, X.L., Yu, J.S., Jiang, H., Sun, W.C., Li, Z.J., 2016. Roles of soil erodibility, rainfall erosivity and land use in affecting soil erosion at the basin scale. *Agric. Water Manag.* 174, 82–92.
- Zeng, L.Y., Wang, M.H., Li, C.M., 2011. Study on soil erosion and its spatio-temporal change at Hongfeng Lake watershed based on RUSLE model. *Hydrogeo. Eng. Geol.* 38 (2), 113–118 (in Chinese).
- Zeng, C., Wang, S.J., Bai, X.Y., Li, Y.B., Tian, Y.C., Li, Y., Wu, L.H., Luo, G.J., 2017. Soil erosion evolution and spatial correlation analysis in a typical karst geomorphology using RUSLE with GIS. *Solid Earth Discuss.* 8 (4), 721–736.
- Zhang, X.B., Wang, S.J., Cao, J.H., Wang, K.L., Meng, T.Y., Bai, X.Y., 2010. Characteristics of water loss and soil erosion and some scientific problems on karst rocky desertification in Southwest China karst area. *Carsologica Sinica* 29 (3), 274–279 (in Chinese).
- Zhang, H.M., Yang, Q.K., Li, R., Liu, Q.R., Moore, D., He, P., Ritsema, C.J., Geissen, V., 2013. Extension of a GIS procedure for calculating the RUSLE equation LS factor. *Comput. Geosci.* 52, 177–188.
- Zheng, W., Wang, Z.M., 2016. Laboratorial simulation influences of different rainfall intensities on soil erosion in karst area, China. *Res. Soil Water Conserv.* 23 (6), 333–339 (in Chinese).